Chemistry & Biology, Vol. 9, 93–101, January, 2002, ©2002 Elsevier Science Ltd. All rights reserved. PII S1074-5521(01)00097-7

Effects of Novel Taxanes SB-T-1213 and IDN5109 on Tubulin Polymerization and Mitosis

Mary Ann Jordan,[1,4] Iwao Ojima,[2] Francisco Rosas,[1] Mariagrazia Distefano,[3] Leslie Wilson,[1] Giovanni Scambia,[3] and Cristiano Ferlini[3]

[1]Department of Molecular, Cellular, and Developmental Biology and The Neuroscience Research Institute
University of California Santa Barbara
Santa Barbara, California 93106

[2]Department of Chemistry
State University of New York at Stony Brook
Stony Brook, New York 11794

[3]Department of Obstetrics and Gynecology
Università Cattolica Sacro Cuore
00165 Rome
Italy

Summary

SB-T-1213 and IDN5109 are semisynthetic, orally available taxanes that are up to 400-fold more active than paclitaxel against drug-resistant cells. IDN5109 is in clinical trials. We investigated the primary target for SB-T-1213 and IDN5109 and whether the compounds interact with microtubules differently than paclitaxel. Unlike paclitaxel, at 1–10 μM both novel taxanes initiate microtubule polymerization in vitro with no lag. They enhance polymerization equally or more potently than paclitaxel. SB-T-1213 induces unusual microtubules with attached extra protofilaments or open sheets, and IDN5109 induces large protofilamentous sheets. Both inhibit HeLa cell proliferation, block mitosis at the metaphase/anaphase transition, bundle microtubules at high drug concentrations, and induce abnormal metaphase spindles and apoptosis. They target microtubules but alter their polymerization and structure differently than paclitaxel. These differences may play a role in their enhanced cytotoxicity and efficacy.

Introduction

Taxanes are among the most important cancer chemotherapeutic agents to have been developed in recent times. Although they are effective in the treatment of many types of cancer, including carcinomas of the ovary, lung, head and neck, bladder, and esophagus [1], their therapeutic use is often associated with undesired toxic side effects as well as the development of multidrug resistance (MDR) [2]. Thus, two analogs were synthesized with the goal of developing taxanes that were more water-soluble and more active in MDR-expressing cancer cells. The two new analogs described here, SB-T-1213 and IDN5109, show significantly higher antitumor activity in MDR-bearing tumor cells than the classic taxane, paclitaxel, as well as greater aqueous solubility and the maintenance of high potency in non-MDR-expressing cancer cells [3–9].

The two novel taxanes, SB-T-1213 and IDN5109 (Figure 1), were synthesized from 10-deacetylbaccatin III and 14β-hydroxy-10-deacetylbaccatin III isolated from *Taxus baccata* and *Taxus walichiana Zucc*., respectively. SB-T-1213 differs from paclitaxel (Figure 1) at the 10 and 3′ positions, and IDN5109 differs from paclitaxel at the 3′ and 1,14 positions. Because such structural alterations could change the primary mechanism of action, it was necessary to determine whether these compounds have similar effects on tubulin, microtubules, and cell functions as does the prototype taxane, paclitaxel.

Paclitaxel binds reversibly to microtubules in vitro, stimulates microtubule polymerization, and promotes both the nucleation and elongation phases of the polymerization reaction [10]. Suppressing microtubule dynamic instability and treadmilling, the drug strongly stabilizes microtubules [11, 12]. It increases the microtubule polymer mass at high concentrations by suppressing tubulin dissociation at microtubule ends while the ends remain free for tubulin addition [12]. High concentrations of paclitaxel have the unique ability to cause microtubules to arrange into parallel bundles in cells [13]. However, at low concentrations paclitaxel strongly inhibits cell proliferation by blocking cell cycle progression specifically at the metaphase/anaphase transition while exerting no discernible effects on the microtubule polymer mass and only subtle effects on mitotic spindle microtubule organization, ultimately leading to apoptosis [14–16].

SB-T-1213 is 135-fold more active than paclitaxel against MCF-7-R cells, a doxorubicin-resistant cell line that expresses the multidrug resistance gene MDR, and it is 5- to 11-fold more effective than paclitaxel against a number of other human cell lines and human tumor xenografts [3, 6]. It inhibits the function of the MDR-associated Pgp-efflux pump [6], is orally available, and is currently undergoing extensive animal studies.

IDN5109, currently in clinical trials, is as much as 440-fold more active than paclitaxel against adriamycin-resistant and vinblastine-resistant breast and leukemia cells [4, 6], is orally active in tumor models with excellent bioavailability (48%–50.5%), appears to have reduced neuro- and other toxicities, and has recently been shown to act as a Pgp reversal agent [7–9].

As a result of the promising activities of SB-T-1213 and IDN5109, we have investigated their interactions with microtubules in vitro and in cells. We find that both novel taxanes enhance the polymerization of bovine brain tubulin in vitro as well as or more potently than paclitaxel but that they induce the formation of unusual tubulin polymers, suggesting that they bind to and affect the conformation and polymerization of tubulin differently than paclitaxel. In HeLa cells, the novel drugs induce aberrant mitotic spindles, block mitosis at the transition from metaphase to anaphase, induce microtubule bundling at high concentrations, and induce apoptosis.

[4]Correspondence: jordan@lifesci.ucsb.edu

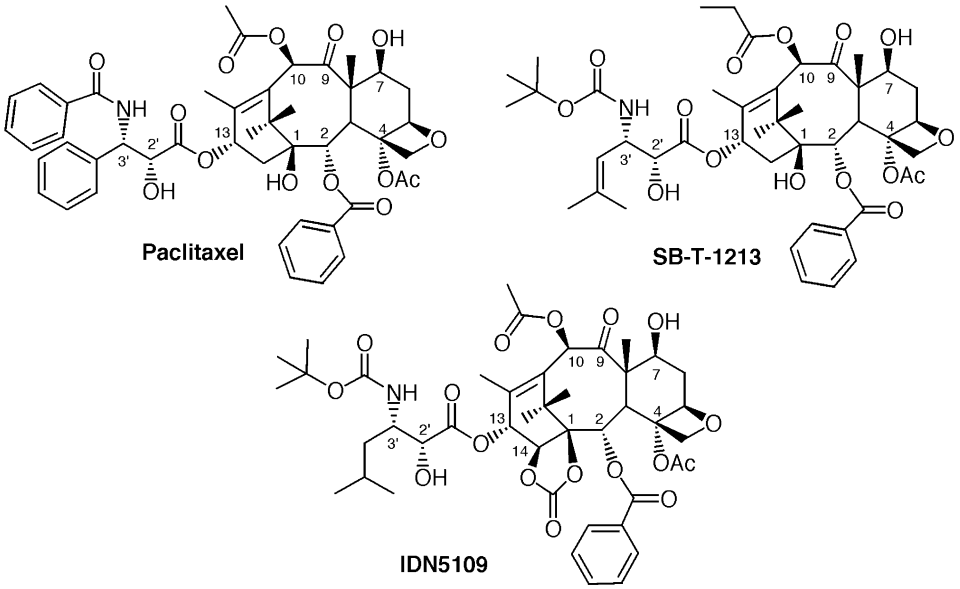

Figure 1. Structural Formulas of SB-T-1213, IDN5109, and Paclitaxel

The results indicate that although these compounds interact somewhat differently with tubulin and its polymers, they share the basic microtubule-targeted antitumor mechanism of the taxanes but have, in addition, the capacity to overcome multidrug resistance.

Results

SB-T-1213 and IDN5109 Induced Polymerization of Tubulin In Vitro More Potently Than Paclitaxel

SB-T-1213 and IDN5109 both stimulated polymerization of tubulin more potently than paclitaxel. Figure 2A shows a representative time course of bovine brain tubulin assembly as measured turbidimetrically in the presence of 1 and 10 μM of the three taxanes. In the control, no significant tubulin polymerization occurred (lowest curve) because the tubulin concentration was at or below the critical concentration for polymerization. At 10 μM (upper three curves), turbidity increased immediately upon the addition of either SB-T-1213 (dashed line) or IDN5109 (solid line) to tubulin, whereas a slight lag occurred after the addition of paclitaxel (dotted line). At 10 μM, SB-T-1213 and IDN5109 enhanced turbidity 58% and 24% more, respectively, than paclitaxel (mean of 3–4 experiments). At a lower concentration (1 μM), SB-T-1213 (lower dashed line) and IDN5109 (lower solid line) enhanced turbidity 112% and 75% more, respectively, than paclitaxel (lower dotted line). Even with lower concentrations of SB-T-1213 and IDN5109 (1 μM), there was no lag before the onset of polymerization, whereas with 1 μM paclitaxel the lag was 3–5 min.

The polymers induced by each of the three drugs were stable in cold to approximately the same degree. After at least 20 min of cooling on ice, 71%–88% of the turbidity induced by 10 μM of each of the three drugs and 30%–40% of the turbidity induced by 1 μM of each of the three taxanes remained (data not shown).

The mass of polymerized tubulin was also determined by sedimentation, a method that is independent of differences in the shape of the polymers formed. Bovine brain tubulin (1.0–1.4 mg/ml, 0.1 mM GTP, 37°C) was incubated with a range of concentrations of SB-T-1213, IDN5109, or paclitaxel (10 nM–3 μM) for 20 min, and the resulting polymer was collected by centrifugation (Experimental Procedures). The extent of polymerization was determined by measuring the reduction in soluble tubulin in the supernatant and comparing it with control supernatants, as shown in Figure 2B. Both the novel taxane analogs and paclitaxel increased the amount of polymerized tubulin in the pellets (reduced the soluble tubulin) in concentration-dependent manners. SB-T-1213 was 30% more potent than paclitaxel at reducing the tubulin remaining in the supernatant, whereas IDN5109 was equivalent in potency to paclitaxel. The EC_{50} value for reduction in soluble tubulin was 0.07 μM for SB-T-1213, as compared with 0.10 μM for both IDN5109 and paclitaxel.

We examined whether the assembly induced by high concentrations of SB-T-1213 and IDN5109 yielded authentic microtubule polymers, as opposed to non-specific drug/tubulin aggregates or precipitates, by using negative-stain electron microscopy. As shown in Figures 3A–3D, both novel taxanes induced the formation of protofilamentous polymers. With IDN5109 (1–10 μM), the predominant polymers were loops or thick fibers of a few or many protofilaments (arrows in Figure 3A), large protofilamentous sheets of varying width (sometimes as large as 30 protofilaments in width) (arrows in Figure 3B), and only rare microtubules. With SB-T-1213 (1–10 μM), microtubules generally predominated; however, a large number of the microtubules had several extra protofilaments or partial microtubules associated linearly (asterisks in Figure 3D), coils of several protofilaments ("C"), or significant sections of unclosed sheet (arrows in Figures 3C and 3D). In contrast, with paclitaxel (1–10 μM), microtubules ("M"; Figures 3E and 3F) were by far

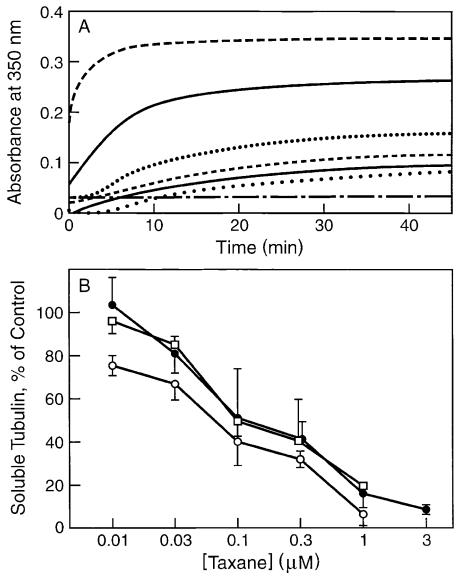

Figure 2. Enhancement of Tubulin Polymerization by SB-T-1213, IDN5109, and Paclitaxel

(A) Time course of polymerization as measured by turbidimetry at 350 nm. Dashed lines represent SB-T-1213 at 10 μM (upper) and 1 μM (lower); solid lines represent IDN5109 at 10 μM (upper) and 1 μM (lower); and dotted lines represent paclitaxel at 10 μM (upper) and 1 μM (lower). The flat line with alternating dots and dashes represents the control. Polymerization was conducted as described in the Experimental Procedures with 13–14 μM tubulin and the indicated drug concentration.

(B) Unpolymerized tubulin remaining after incubation with each of the three taxanes is presented as a percentage of unpolymerized tubulin in controls (no drug). In other words, the graph shows the concentration dependence for reduction in soluble tubulin by IDN5109, SB-T-1213, and paclitaxel as measured by the sedimentation of polymer. Tubulin (10–14 μM) was incubated with a range of concentrations of the three taxanes (SB-T-1213, open circles; IDN5109, closed circles; paclitaxel, open squares) at 37°C for 20 min and centrifuged to sediment polymer (Experimental Procedures). Tubulin remaining in the supernatants was compared with tubulin in supernatants of reaction mixtures incubated in the absence of a drug. Without a drug, there was no reduction in soluble protein after centrifugation, and no visible pellet formed. Results are presented as a percent of control supernatant protein values and are the mean and SE of four independent experiments.

the predominant form, and only a few sheets and loops were formed. Thus, SB-T-1213 induced a greater polymer mass than paclitaxel, and the polymers were somewhat less normal. IDN5109 induced the same polymer mass as paclitaxel by sedimentation, but the polymers were extremely aberrant.

SB-T-1213 and IDN5109 Inhibited HeLa Cell Proliferation More Potently Than Paclitaxel

To determine whether the effects of the novel taxanes on microtubule polymerization resulted in differences in their cellular mechanisms of action, we examined their actions in HeLa cells, a cell line for which we have extensive experience with paclitaxel. Proliferation was inhibited by 50% (IC_{50}) at concentrations of 2.3 ± 0.6 nM with SB-T-1213, 1.8 ± 0.5 nM with IDN5109, and 4.8 ± 0.9 nM with paclitaxel (72 hr). Clonogenic assays indicated the absence of additional long-term effects; clonogenicity was inhibited at concentrations of 1.1 ± 0.6 nM with SB-T-1213, 1.9 ± 0.8 nM with IDN5109, and 3.7 ± 1.1 nM with paclitaxel. Thus the IC_{50} values for inhibition of clonogenicity were very similar to those obtained in the short-term growth inhibition experiments.

SB-T-1213 and IDN5109 Blocked Cell-Cycle Progression at the Metaphase/Anaphase Transition

The mitotic index was determined after a 20 hr incubation with a range of concentrations of the novel compounds. As shown in Figure 4 (left axis, open circles), SB-T-1213 at 6 nM induced 50% mitotic block, and 30 nM induced 90% mitotic block. With IDN5109, 10 nM induced 50% mitotic block and 60 nM induced 90% mitotic block (open squares). We previously found that 8 nM paclitaxel induced 50% mitotic block in HeLa cells, and 30–100 nM induced 80%–90% mitotic block [14].

We examined the ratio of cells in anaphase to cells in metaphase to determine if, like paclitaxel, the novel taxanes block mitosis specifically at the transition from metaphase to anaphase. As shown in Figure 4 (right axis, filled symbols), the anaphase/metaphase ratio decreased in a concentration-dependent manner, from 0.31 in controls (in the absence of compound) to 0.03 at 3 nM SB-T-1213 and 0.05 at 3 nM IDN5109. No cells were detected in anaphase at concentrations of more than 10 nM for SB-T-1213 or IDN5109. Paclitaxel gave similar results; the anaphase/metaphase ratio decreased to 0.01 at 10 nM drug, and no cells were detected in anaphase at higher concentrations [14].

Low Concentrations of SB-T-1213 and IDN5109 Induced Abnormal Spindle and Nuclear Morphology

Very low concentrations of the taxane analogs induced distinct disruptions of microtubule spindle morphology and nuclear organization that strongly resembled those induced by paclitaxel. In control HeLa cells in metaphase, spindles were bipolar with a compact, dense plate of condensed chromosomes (Figures 5A and 5B). Very low concentrations of either analog (as low as 1 nM) induced the formation of predominantly multipolar multiastral spindles with disorganized arrays of chromosomes (Figures 5C–5F). In bipolar spindles, individual chromosomes were frequently associated with only one spindle pole, indicating that the chromosomes were unable to achieve a normal bipolar attachment to the spindle and thus were unable to congress to the metaphase plate (Figures 5C and 5D).

High Concentrations of SB-T-1213 and IDN5109 Induced Microtubule Bundling in Cells

In control HeLa cells during interphase, microtubules formed a fine network of unaligned microtubules (Figure 6A). As shown in Figures 6B and 6C, 10 nM SB-T-1213 and 30 nM IDN5109 induced the formation of small, loose bundles of parallel microtubules. At more than 30 nM of either compound, microtubule bundles were large, compact, and prominent (data not shown). Thus, like paclitaxel, at high concentrations both novel taxanes

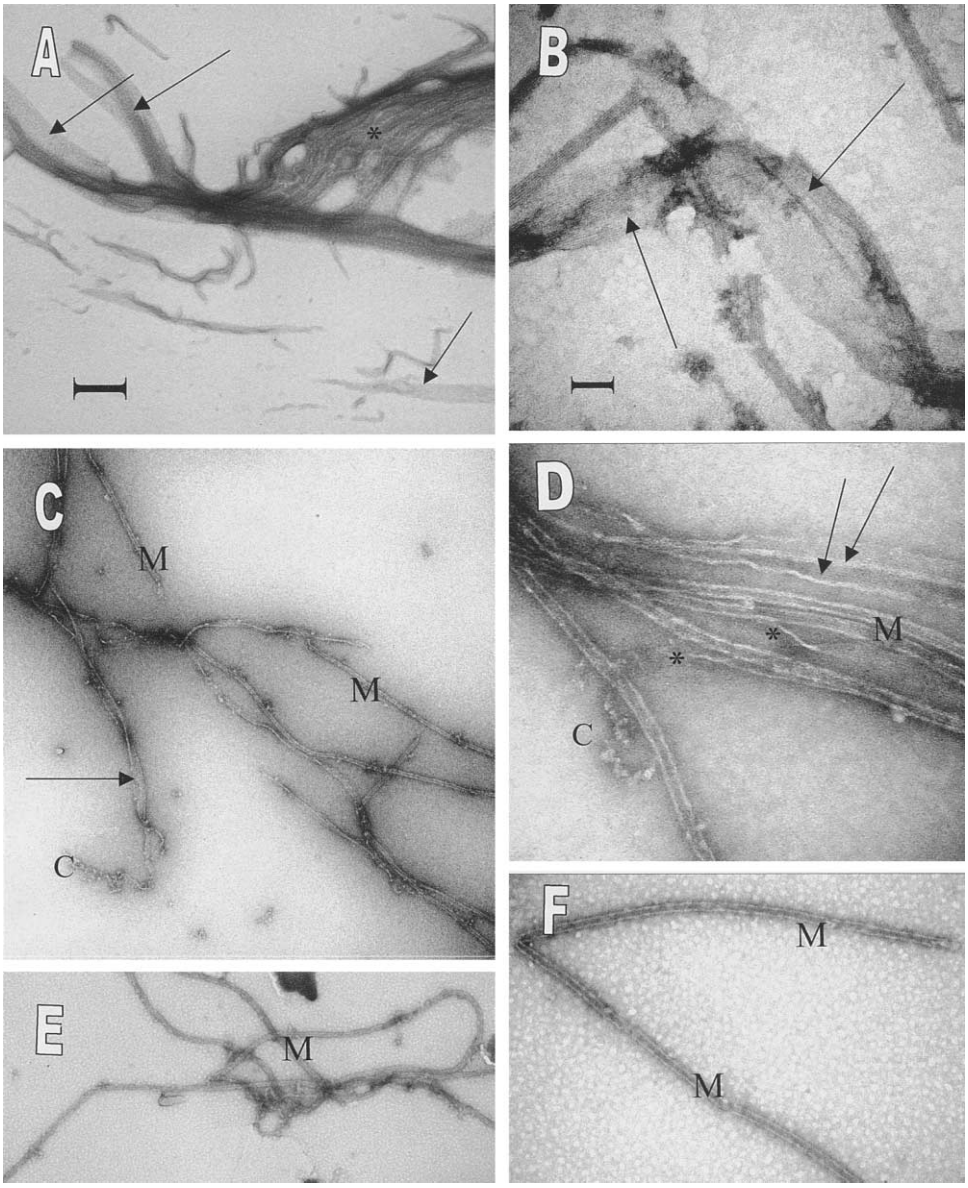

Figure 3. Tubulin Polymers Induced by 1 μM IDN5109 or 1 μM SB-T-1213, as Compared with Paclitaxel

Electron micrographs; left column, low magnification; right column, high magnification. IDN5109 (A and B) induced the formation of large bundles of fibers (asterisk), large sheets (arrows), and a few microtubules. SB-T-1213 (C and D) induced the formation of microtubules (M) and a few sheets (arrows), partial microtubules, loops and coils (C), and long regions of a small number of protofilaments associated linearly with microtubules. Paclitaxel (1 μM) (E and F) induced the formation of many microtubules (M) and few sheets or loops. The scale bar in (A) represents 500 nm; that in (B) represents 100 nm. (A), (C), and (E) are at the same magnification, as are (B), (D), and (F).

induced formation of bundles of microtubules or tubulin polymers (see below).

An important characteristic of paclitaxel's actions is that many cells become multinucleate after incubation for 20 hr with low concentrations of the drug (Table 1; [16]). This phenomenon occurred to an even greater degree with the two novel taxane analogs; that is, the proportions of multinucleate cells reached levels as high as 60% and 70% (Table 1). In control cells in interphase, only 2.7 ± 0.6% contained more than one nucleus. At concentrations of SB-T-1213 as low as 0.3 nM and at concentrations of IDN5109 as low as 1 nM, large numbers of interphase cells were multinucleate (32.6% and 29.9%, respectively). The proportion of multinucleated interphase cells increased with increasing compound concentration, reaching levels greater than 70% and greater than 60% at 10–30 nM SB-T-1213 and IDN5109, respectively. The proportions of multinucleated cells decreased at concentrations of more than 30 nM SB-T-1213 or IDN5109 and more than 10 nM paclitaxel.

At the lowest concentrations (0.3–1 nM), multinucleated cells contained from 2 to 4 nuclei, whereas at more than 3 nM, the number of nuclei was often as great as 5–10 per cell. In addition, after incubation for 20 hr with

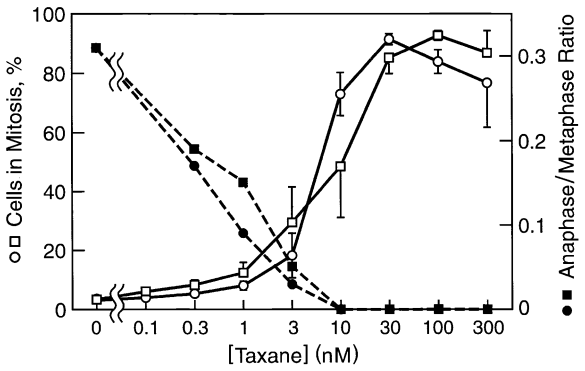

Figure 4. Taxane Concentration Dependence for Mitotic Arrest and Block at the Metaphase/Anaphase Transition

Mitotic index (left axis; SB-T-1213, open circles; IDN5109, open squares); ratio of cells in anaphase to cells in metaphase (right axis; SB-T-1213, filled circles; IDN5109, filled squares). HeLa cells were incubated with taxane for 20 hr, then fixed and stained for microtubules and chromatin (Experimental Procedures). The numbers of cells in metaphase and anaphase were counted by microscopy. Values are the mean ± SE of 4–5 experiments and represent counts from at least 50 mitotic cells/concentration in each experiment and 100 interphase cells/concentration per experiment.

3 nM of either analog, the sizes of the resulting cells varied considerably, and occasionally, grape-like clusters of attached small cells occurred. These clusters appeared to result from incomplete cytokinesis (Figures 5E and 5F). Cell clustering, the varying sizes of cells, multinucleation, and the abnormality of nearly all spindles suggested that many cells underwent an abnormal mitosis and reentered interphase without completing cytokinesis, as observed previously with paclitaxel [16]. The decrease in the proportion of multinucleated cells at higher drug concentrations may result from a more potent and enduring mitotic block in the presence of high drug concentrations.

SB-T-1213 and IDN5109 Induced Apoptosis at the Same Concentrations That Induced Mitotic Block

By TUNEL assay, as shown in Figure 7A, incubation of HeLa cells with the novel taxanes at concentrations as low as 2.5 nM for 24 hr induced apoptosis. Higher concentrations of paclitaxel (5 nM; Figure 7B) were required for induction of apoptosis. The percentage of cells that were apoptotic reached 70% with 5 nM SB-T-1213 and 40% with 5 nM IDN5109 at 24 hr. These data indicate that apoptosis was strongly correlated with mitotic block.

Figure 8 shows the 24 hr time course for induction of apoptosis by 5 nM SB-T-1213 as determined by flow cytometry analysis that combined results of the TUNEL assay (anti-BrDu FITC fluorescence) with the assay of cellular DNA content. The numbers in the lower right of each panel indicate the percentage of cells that were apoptotic (having high anti-BrDu FITC fluorescence and lying above the diagonal line). The data indicate that most apoptotic cells arise from cells that remain blocked in the G2/M stage of the cell cycle or from cells blocked in G2/M that subsequently reenter interphase without undergoing cytokinesis.

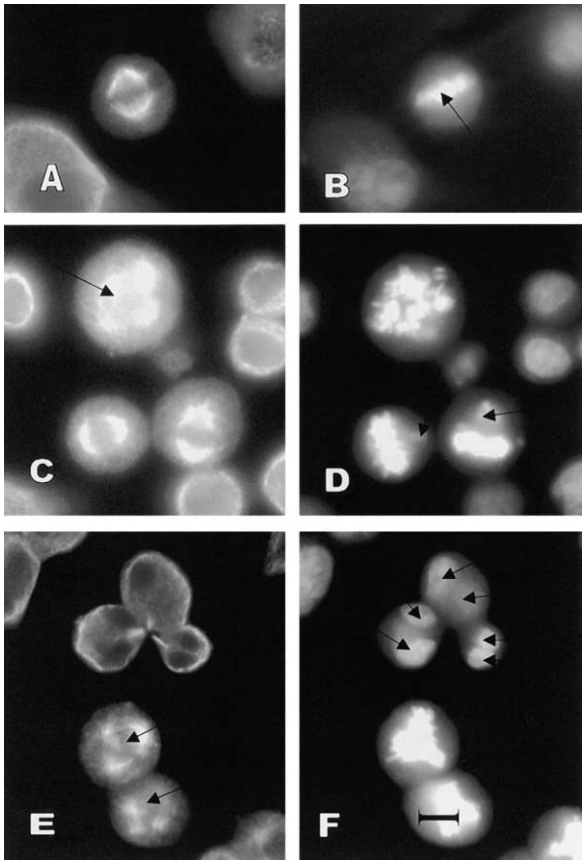

Figure 5. Induction of Abnormal Spindles by SB-T-1213 and IDN5109

HeLa cells incubated with no drug (A and B), 1 nM SB-T-1213 (C and D), or 3 nM IDN5109 (E and F) for 20 hr, followed by fixation and staining for tubulin (A, C, and E) and chromosomes (B, D, and F). In the absence of drug (A and B), metaphase spindles are bipolar with compact metaphase plates of chromosomes (arrow). At low concentrations of SB-T-1213 (1 nM), spindles are bipolar or multipolar (arrow in C), and chromosomes often fail to congress to the metaphase plate and instead remain at the poles (arrows in D). At low concentrations of IDN5109, similar abnormalities occur. Two multipolar spindles (arrows in E) as well as one cluster of three small cells resulting from an aberrant incomplete cytokinesis (arrows in F) are shown in (E) and (F). The resulting cells are multinucleate (arrows in F). The scale bar represents 10 μm.

Discussion

We find that SB-T-1213 and IDN5109 induce tubulin polymerization significantly differently from paclitaxel, both in the rate and extent of polymerization and in the morphology of the polymers formed. SB-T-1213 stimulated tubulin polymerization in vitro with little or no lag of initiation (Figure 2A). By turbidimetry, SB-T-1213 (1 and 10 μM) enhanced polymerization by 58% and 112%, respectively, more than paclitaxel. By sedimentation, SB-T-1213 was 30% more potent than paclitaxel in reducing the concentration of soluble tubulin (Figure 3B). Thus, it is clear by both methods of measuring polymer mass that SB-T-1213 induces tubulin polymerization significantly more than paclitaxel. Microtubules were the predominant product of the induced assembly reaction,

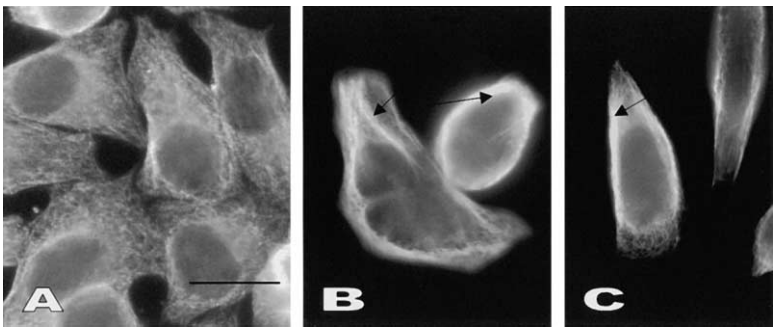

Figure 6. Microtubule Bundling Induced by High Concentrations of SB-T-1213 and IDN5109

Control HeLa cells (A) exhibit a normal meshwork of fine microtubules in interphase. After a 20 hr incubation with 30 nM SB-T-1213 (B) and 30 nM IDN5109 (C), bundles of microtubules are clearly evident (arrows). The scale bar represents 22 μm.

although sheets and partial microtubules were also commonly formed (Figure 3). Paclitaxel also induced the formation of sheets, but they were fewer in number than with SB-T-1213 and the microtubules induced by paclitaxel were of normal appearance, rather than having partial microtubules or extra protofilaments associated with them.

IDN5109 also potently stimulated tubulin polymerization in vitro with no detectable lag. The turbidimetric signal reached significantly higher levels than with paclitaxel (1 and 10 μM IDN5109, 24% and 75% higher than paclitaxel, respectively; Figure 2A). However, since predominantly large sheets were formed, it is possible that the turbidimetric signal over-represented the true mass of polymer induced by IDN5109. This is supported by the observation that the reduction of soluble tubulin by IDN5109 equals that of paclitaxel in centrifugation experiments (EC_{50} of 0.1 μM for both paclitaxel and IDN5109; Figure 8B). It should be mentioned that it is conceivable that the absence of a lag in initiation of the turbidimetric increase with both novel drugs might reflect a difference in the morphology of the polymer formed at early time points. Overall, we found that both novel taxanes are equal or better than paclitaxel in their ability to enhance tubulin polymerization, with SB-T-1213 exhibiting higher potency than IDN5109.

The marked tendency of IDN5109 and SB-T-1213 to induce polymerization of tubulin into sheets and other aberrant microtubule-like forms, in combination with the more potent stimulation of assembly by SB-T-1213, suggests that the novel taxanes induce conformational changes in tubulin that differ significantly from the conformational changes induced by paclitaxel. Paclitaxel binds with low affinity to soluble vertebrate neuronal tubulin and binds reversibly with high affinity, apparently to the interior surface of microtubules, in a 1:1 stoichiometry with tubulin in the microtubules [17–20]. Paclitaxel preferentially induces microtubules with 12, rather than 13, protofilaments [21, 22]. Thus, paclitaxel appears to induce a slight reduction of the lateral contact curvature between tubulin monomers in the microtubule. In the cold or under rapid assembly conditions, paclitaxel induces the formation of some hoops and sheets as well as microtubules. The observation that SB-T-1213 and IDN5109 induce formation of more non-microtubule polymers than paclitaxel can not be taken as evidence of the intracellular polymer morphology induced by these drugs; rather, the results indicate that these novel drugs interact differently with tubulin and microtubules than paclitaxel. The most potent effect of all three drugs in cells appears to involve mitotic block, which likely results from suppression of microtubule dynamics and leads to apoptosis. The differing effects of the novel taxanes on the polymerization of brain tubulin in vitro indicate that they are likely to affect microtubule polymer formation and dynamics in cells differently than paclitaxel.

We found that SB-T-1213 and IDN5109 inhibited HeLa cell proliferation, blocked mitosis, and induced apoptosis in mitotically blocked cells. They exhibit 2-fold greater ability than paclitaxel to inhibit proliferation, with IC_{50} values of 2.3 nM for SB-T-1213 and 1.8 nM for IDN5109 (Table 1), as compared with an IC_{50} for paclitaxel of 4.8 nM. In addition, they induced apoptosis at concentrations as low as 2.5 nM, whereas paclitaxel required a concentration of 5 nM to induce mitotic block and apoptosis.

Like paclitaxel, at low concentrations (≥0.3 nM) both novel taxanes induced abnormal metaphase spindles with uncongressed chromosomes and inhibited mitosis

Table 1. Effects of SB-T-1213 and IDN5109 (20 hr Incubation) on Induction of Multinucleation in HeLa Cells

	Multinucleate Cells (%)		
Taxane Concentration (nM)	SB-T-1213	IDN5109	Paclitaxel
0 (control)	2.7 ± 0.6	2.7 ± 0.6	2.7 ± 0.7
0.3	32.6 ± 9.2	9.6 ± 0.9	3.2 ± 1.2
1	41.6 ± 7.6	29.9 ± 9.0	11.6 ± 4.0
3	60.4 ± 11.5	49.0 ± 17.5	32.1 ± 17.9
10	71.4 ± 2.1	59.8 ± 8.2	37.7 ± 11.5
30	71.9 ± 5.3	60.4 ± 13.1	16.5 ± 4.5
100	28.1 ± 6.5	31.1 ± 19.1	14.0 ± 6.8
300	49.9 ± 22.1	23.9 ± 10.0	n.a.

Mean and standard error of the mean for n = 2–3 experiments. Data for paclitaxel are from [14].

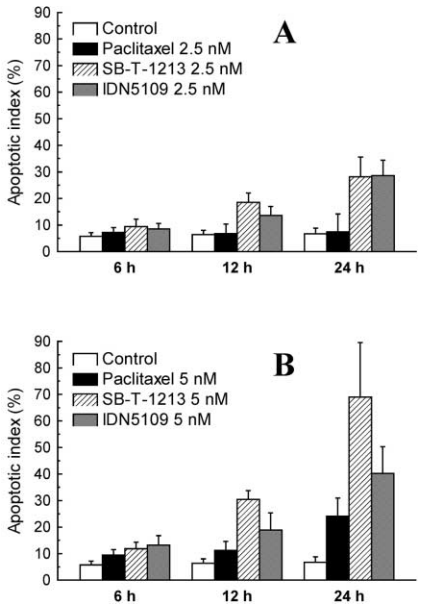

Figure 7. Time Course for Induction of Apoptosis by SB-T-1213, IDN5109, and Paclitaxel
(A) 2.5 nM drug.
(B) 5 nM drug.
Apoptosis was measured by a TUNEL assay (see Experimental Procedures). Error bars represent SD.

specifically at the transition from metaphase to anaphase. In this respect the mechanisms of SB-T-1213 and IDN5109 resemble those of a number of microtubule-targeting drugs, including paclitaxel, vinca alkaloids, colchicine, nocodazole, podophyllotoxin, dolastatin analogs, and the cryptophycins [23]. In addition, at somewhat higher concentrations (≥10–30 nM), both novel taxanes induced bundling of microtubules in interphase that resemble the bundles induced by paclitaxel [10, 14].

The novel taxanes also induced the formation of very large numbers of multinucleated interphase cells (Table 1; Figures 5 and 6). For example, the percentage of multinucleated interphase cells at a 10 nM concentration of each drug was 71.4 ± 2.1% with SB-T-1213 and 59.8 ± 8.2% with IDN5109. By comparison, the highest proportion of multinucleated interphase cells observed with paclitaxel was 37.7 ± 11.5%, also at a concentration of 10 nM (20 hr incubation) [14]. Multinucleate cells appear to be formed when mitotically blocked cells revert to interphase without completing cytokinesis [14, 16]. In addition, the appearance of clusters of small attached cells (Figure 6) is also indicative of faulty cytokinesis. Mitotic block, formation of aberrant spindles and multinucleated interphase cells, and induction of apoptosis all occur at concentrations of SB-T-1213 and IDN5109 that are similar to the concentrations that inhibit cell proliferation, suggesting that, as with paclitaxel, their primary mechanism is blockage and disruption of mitosis by suppression of microtubule dynamics.

Significance

SB-T-1213 and IDN5109 are semisynthetic, orally available taxanes that are up to 400-fold more active than paclitaxel against several drug-resistant cell lines. Their potency combined with their improved aqueous solubility, oral availability, and remarkable lack of susceptibility to multidrug resistance mechanisms indicates that they are strong candidates for efficacious antitumor agents. SB-T-1213 and IDN5109 affect tubulin polymerization and microtubule structure differently from the classic taxane, paclitaxel, and they are more potent than paclitaxel, even in cells such as HeLa that are not multidrug resistant. In contrast to paclitaxel, at 1–10 μM both novel taxanes initiate microtubule polymerization in vitro with no turbidimetric lag and enhance polymerization equally or more potently. SB-T-1213 induces the formation of unusual microtubules with attached extra protofilaments or open sheets, and IDN5109 induces large protofilamentous sheets. The marked tendency of IDN5109 and SB-T-1213 to induce the polymerization of tubulin into sheets and other aberrant microtubule-like forms, in combination with the more potent stimulation of assembly by SB-T-1213, suggests that the novel taxanes induce conformational changes in tubulin that differ significantly from the conformational changes induced by paclitaxel. These differences in their interactions with tubulin and microtubules may play a direct role in their enhanced cytotoxic potency and antitumor efficacy. Their inhibition of HeLa cell proliferation, induction of mitotic block with abnormal spindle formation, bundling of microtubules at high drug concentrations, and timing of induction of apoptosis from cells blocked in mitosis all indicate that, like paclitaxel, their principal target in tumor cells is microtubules.

Experimental Procedures

Tubulin Purification and Microtubule Assembly

Bovine brain tubulin was purified by three cycles of polymerization and depolymerization, followed by phosphocellulose chromatography, and stored frozen at −70°C [24]. The ability of the compounds to enhance tubulin polymerization was determined in two ways: (1) tubulin (1.0–1.4 mg/ml) was incubated with a range of drug concentrations in assembly buffer (0.1 M Pipes, 1 mM $MgSO_4$, 1 mM EGTA [pH 6.8]) containing 0.1 mM GTP at 37°C for 20 min followed by centrifugation in a Beckman Coulter Optima MAX ultracentrifuge (150,000 × G, 30 min, 37°C), aspiration of supernatants, and determination of supernatant protein concentration by the method of Bradford [25], with bovine serum albumin used as a standard; and (2) tubulin (1.3–1.4 mg/ml) in assembly buffer containing 1 mM GTP was polymerized in the presence of a range of drug concentrations by warming from 0°C to 30°C in a Gilford Response recording spectrophotometer equipped with a constant-temperature cuvet chamber. Polymerization was quantitated by the measurement of turbidity at 350 nm.

Electron Microscopy

Tubulin (1.1–1.2 mg/ml) was assembled in the presence of drug (1–10 μM) in assembly buffer containing 0.1 mM GTP by warming to 37°C for 30 to 45 min. Samples for electron microscopy were fixed by diluting 1:25 into 0.3% aqueous glutaraldehyde. After 30–60 s fixation, samples (4 μl) were applied to parlodion- or carbon-coated electron microscope grids for 30 s, then drawn off with torn filter paper, followed sequentially by cytochrome C (1 mg/ml) for 20 s, three drops H_2O, and 1% uranyl acetate for 20 s, then viewed in a JEOL 1230 at 80 KV. Results are from two independent experiments.

Cell Culture and Proliferation

HeLa S3 cells from epithelioid carcinoma of human cervix (American Type Culture Collection, Rockville, MD) were grown in monolayer in tissue culture flasks or 35 mm six-well plates (Nunc, Rochester,

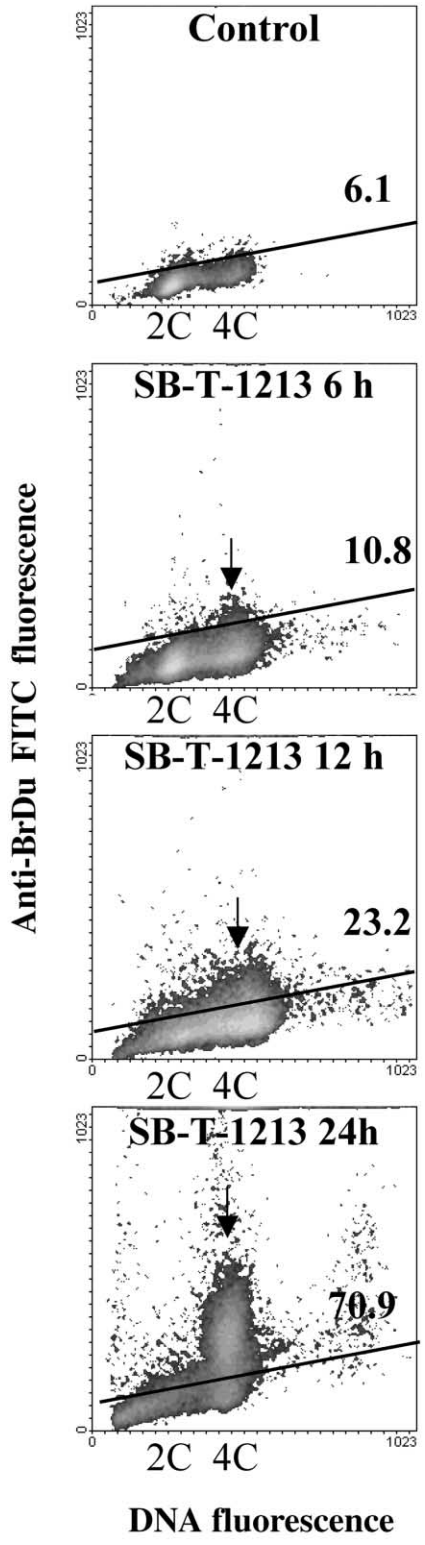

Figure 8. Time Course for the Induction of Apoptosis by 5 nM SB-T-1213

Results of a TUNEL assay (anti-BrDu FITC fluorescence) in combination with an assay of the amount of DNA, both by flow cytometry. The time of drug incubation varied from 0 to 24 hr and is indicated at the top of each panel. The percentage of apoptotic cells is indicated in the lower right of each panel. The peak of apoptotic cells is associated with the 4C region of DNA, indicating that apoptosis occurred in cells blocked in G2/M or cells that reverted to interphase from G2/M without undergoing cytokinesis.

NY; Falcon, Becton Dickinson, Lincoln Park, NJ; Corning, Corning, NY) in Dulbecco's modified Eagle's medium supplemented with 10% fetal bovine serum (Sigma Chemical Co., St. Louis, MO) at 37°C in 5% CO_2, in the absence of antibiotics. Cells were plated in six-well flat-bottom plates (Falcon, Lincoln Park, NJ) at a concentration of 10^5 cells/ml in complete medium. After 24 hr, the medium was replaced with media containing the test compounds (concentration range 0.1–50 nM). Control cells were treated with vehicle alone. After 20 hr of drug exposure, cells were washed twice and then cultured in the absence of taxanes for an additional 48 hr. At this time, viable adherent cells were counted four times (two experiments by two independent operators) with a Diavert inverted microscope (Leica, Wetzlar, Germany).

Clonogenic Assay

Approximately 0.8×10^3–1×10^3 cells were seeded into triplicate 25 cm^2 flasks and incubated with a range of drug concentrations (0.1-10 nM) for 20 hr. Flasks were then gently washed with PBS, replaced with fresh medium, and incubated at 37°C. After 10–12 days, cells were fixed and stained with 1% methylene blue in 70% ethanol, and colonies were evaluated by visual count. The number of colonies in treated cultures was expressed as a percentage of the control cultures. All results represent means and standard deviations from at least three independent experiments.

Immunofluorescence Microscopy

Subcultures of cells were seeded in 35 mm dishes containing #1.5 glass coverslips freshly coated with polylysine (50 μg/ml, 2 hr, 37°C, followed by rinsing with sterilized deionized water). After drug incubation, adherent cells were fixed in 10% formalin in PBS (2.7 mM potassium chloride, 2.93 mM potassium phosphate monobasic, 137 mM sodium chloride, 14 mM dibasic sodium phosphate, 7.69 mM sodium azide, 2 mM EGTA [pH 7.2–7.4]) at 25°C for 10 min, then transferred to 99.6% methanol, 2 mM ethylene glycol bis (B-aminoethyl ether)-N,N,N′N′-tetraacetic acid (−20°C) for 10 min. After blocking of nonspecific antibody binding with normal goat serum, fixed cells were stained for tubulin with a mouse monoclonal antibody (DM1A, Sigma), followed by fluorescein isothiocyanate-conjugated goat anti-mouse immunoglobulin G (Cappel, West Chester, PA), and DAPI (4,6-diamidino-2-phenylindole) for chromosomes. a Nikon Eclipse microscope with a 60× oil immersion objective, a Hamamatsu Orca II CCD camera, and a Metamorph Imaging system were used to obtain photomicrographs by epifluorescence.

Mitotic Index

HeLa cells were seeded at a density of 2×10^4–4×10^4 cells/ml in 35 mm six-well plates. After 2 days, media were replaced with fresh media containing compound. Twenty hr later, both attached and floating cells were collected and combined (by trypsinization and centrifugation), and cells were fixed and stained as described above, except that cells were collected after each step by centrifugation (3 min, clinical centrifuge) and cell pellets were resuspended in fixative, stain, or washing buffer in the order described above. Mitotic indices were determined by counting cells by microscopy.

Apoptosis and DNA Analysis

HeLa cells were plated at a concentration of 10^5 cells/ml as described above. After 24 hr, medium was replaced with fresh medium containing either the compound to be tested or vehicle alone. After incubation with compound (6–24 hr), cells were harvested, and nuclei were isolated and stained for DNA with 0.1% Na^+citrate, 0.1% NP40, 4 mM EDTA, and 50 μg/ml propidium iodide [26] for 12 or more hours at 4°C. d-UTP labeling of DNA strand breaks was performed with the Apodirect kit (Pharmingen, San Diego, CA) according to the manufacturer's directions. Flow cytometric DNA analysis was performed on 2×10^4 or more nuclei with a Facscan flow cytometer (Becton Dickinson, San Jose, CA). DNA fluorescence was

collected in linear mode, and pulse signal processing was used to set a doublet discrimination gate. Cell cycle analysis was performed in two independent experiments with a Multicycle software package (Phoenix, San Diego, CA).

Acknowledgments

We gratefully acknowledge the technical assistance of Sean Nasri and Kathryn Smith, as well as the expert purification of bovine brain tubulin by Herb Miller. This work was supported by the National Institutes of Health grants CA57291 (to M.A.J. and L.W.) and GM42798 (to I.O.).

References

1. Rowinsky, E. (1997). The development and clinical utility of the taxane class of antimicrotubule chemotherapy agents. Annu. Rev. Med. *48*, 353–374.
2. Arbuck, S. (1995). Paclitaxel: current developmental approaches of the National Cancer Institute. Seminars in Oncology Suppl 15 *22*, 55–63.
3. Ojima, I., Slater, J.C., Michaud, E., Kuduk, S.D., Bounaud, P.-Y., Vrignaud, P., Bissery, M.C., Veith, J.M., Pera, P., and Bernacki, R.J. (1996). Syntheses and structure-activity relationships of the second-generation antitumor taxoids: exceptional activity against drug-resistant cancer cells. J. Med. Chem. *39*, 3889–3896.
4. Distefano, M., Scambia, G., Ferlini, C., Gaggini, C., De Vincenzo, R., Riva, A., Bombardelli, E., Ojima, I., Fattorossi, A., Panici, P., et al. (1997). Anti-proliferative activity of a new class of taxanes (14beta-hydroxy-10-deacetylbaccatin III derivatives) on multidrug-resistance-positive human cancer cells. Int. J. Cancer *72*, 844–850.
5. Ferlini, C., Distefano, M., Pierelli, L., Bonanno, G., Riva, A., Bombardelli, E., Ojima, I., Mancuso, S., and Scambia, G. (1999). Cytotoxic effects toward human hematopoietic progenitor cells and tumor cell lines of paclitaxel, docetaxel, and newly developed analogues IDN5109, IDN5111, and IDN5127. Oncol. Res. *11*, 471–478.
6. Ferlini, C., Distefano, M., Pignatelli, F., Lin, S., Riva, A., Bombardelli, E., Mancuso, S., Ojima, I., and Scambia, G. (2000). Antitumour activity of novel taxanes that act as cytotoxic agents and P-glycoprotein inhibitors at the same time. Br. J. Cancer *83*, 1762–1768.
7. Polizzi, D., Pratesi, G., Tortoreto, M., Supino, R., Riva, A., Bombardelli, E., and Zunino, F. (1999). A novel taxane with improved tolerability and therapeutic activity in a panel of human tumor xenografts. Cancer Res. *59*, 1036–1040.
8. Nicoletti, M., Colombo, T., Rossi, C., Monardo, C., Stura, S., Zucchetti, M., Riva, A., Morazzoni, P., Donati, M., Bombardelli, E., et al. (2000). IDN5109, a taxane with oral bioavailability and potent antitumor activity. Cancer Res. *60*, 842–846.
9. Vredenburg, M.R., Ojima, I., Veith, J., Pera, P., Kee, K., Cabral, F., Sharma, A., Kanter, P., and Bernacki, R.J. (2001). Effects of orally-active taxanes on P-glycoprotein modulation colon and breast carcinoma resistance. J. Natl. Cancer Inst., *93*, 1234–1245.
10. Horwitz, S.B. (1992). Mechanism of action of taxol. Trends in Pharmacol. Sci. *13*, 134–136.
11. Wilson, L., Miller, H.P., Farrell, K.W., Snyder, K.B., Thompson, W.C., and Purich, D.L. (1985). Taxol stabilization of microtubule in vitro: dynamics of tubulin addition and loss at opposite microtubule ends. Biochemistry *24*, 5254–5262.
12. Derry, W.B., Wilson, L., and Jordan, M.A. (1995). Substoichiometric binding of taxol suppresses microtubule dynamics. Biochemistry *34*, 2203–2211.
13. Schiff, P.B., and Horwitz, S.B. (1980). Taxol stabilizes microtubules in mouse fibroblast cells. Proc. Natl. Acad. Sci. USA *77*, 1561–1565.
14. Jordan, M.A., Toso, R.J., Thrower, D., and Wilson, L. (1993). Mechanism of mitotic block and inhibition of cell proliferation by taxol at low concentrations. Proc. Natl. Acad. Sci. USA *90*, 9552–9556.
15. Yvon, A.-M., Wadsworth, P., and Jordan, M.A. (1999). Taxol suppresses dynamics of individual microtubules in living human tumor cells. Mol. Biol. Cell *10*, 947–949.
16. Jordan, M.A., Wendell, K.L., Gardiner, S., Derry, W.B., Copp, H., and Wilson, L. (1996). Mitotic block induced in HeLa cells by low concentrations of paclitaxel (Taxol) results in abnormal mitotic exit and apoptotic cell death. Cancer Res. *56*, 816–825.
17. Parness, J., and Horwitz, S.B. (1981). Taxol binds to polymerized tubulin in vitro. J. Cell Biol. *91*, 479–487.
18. Diaz, J.F., and Andreu, J.M. (1993). Assembly of purified GDP-tubulin into microtubules induced by taxol and taxotere: reversibility, ligand stoichiometry, and competition. Biochemistry *32*, 2747–2755.
19. Caplow, M., Shanks, J., and Ruhlen, R. (1994). How taxol modulates microtubule disassembly. Biochemistry *269*, 23399–23402.
20. Nogales, E., Wolf, S.G., Khan, I.A., Luduena, R.F., and Downing, K.A. (1995). Structure of tubulin at 6.5 Å and location of the taxol-binding site. Nature *375*, 424–427.
21. Mogenson, M.M., and Tucker, J.B. (1990). Taxol influences control of protofilament number at microtubule-nucleating sites in Drosophila. J. Cell Sci. *97*, 101–107.
22. Andreu, J.M., Bordas, J., Diaz, J.F., Garcia de Ancos, J., Gil, R., Medrano, F.J., Nogales, E., Pantos, E., and Towns-Andrews, E. (1992). Low resolution structure of microtubules in solution; synchrotron x-ray scattering and electron microscopy of taxol-induced microtubules assembled from purified tubulin in comparison with glycerol and map-induced microtubules. J. Mol. Biol. *226*, 169–184.
23. Jordan, M.A., and Wilson, L. (1998). Microtubules and actin filaments: dynamic targets for cancer chemotherapy. Curr. Opin. Cell Biol. *10*, 123–130.
24. Toso, R.J., Jordan, M.A., Farrell, K.W., Matsumoto, B., and Wilson, L. (1993). Kinetic stabilization of microtubule dynamic instability in vitro by vinblastine. Biochemistry *32*, 1285–1293.
25. Bradford, M.M. (1976). A rapid and sensitive method for the quantitation of microgram quantities of protein utilizing the principle of protein-dye binding. Anal. Biochem. *72*, 248–254.
26. Ferlini, C., Di Cesare, S., Rainaldi, G., Malorni, W., Samoggia, P., Biselli, R., and Fattorossi, A. (1996). Flow cytometric analysis of the early phases of apoptosis by cellular and nuclear techniques. Cytometry *24*, 106–115.